

Novel Anode Materials for Oxygen Evolution during Seawater Electrolysis for Green Hydrogen Fuel Production

A. A. El-Moneim*

*Materials Science and Engineering Department, Egypt-Japan University of Science and Technology,
P.O. Box 179, New Borg El-Arab City, Alexandria, Egypt*

Abstract

$Mn_{1-x-y}Mo_xW_yO_{2+x+y}$ triple oxide electrocatalysts for the anode producing oxygen without forming chlorine in seawater electrolysis were prepared by anodic deposition. The performance of the anode for oxygen evolution in 0.5 M NaCl solutions was examined. The tungsten addition was effective in extending the life of the anode by decreasing the density of pores in electrocatalysts responsible for partial detachment of electrocatalysts, which occurs by high pressure of oxygen formed preferentially at the bottom of pores during electrolysis. Repeated anodic deposition of the electrocatalyst significantly extended the life of the anode, because repeated deposition was able to cover the pores in the underlying electrocatalysts. The potential observed in anodic polarization of an oxide electrode was the sum of the overpotential of the electrochemical reaction and the potential drop as a result of passage of current through the oxide. The potential difference of the two anodes at individual current, ΔE_i , versus the current, i , should show the straight line: The gradient, $\partial \Delta E_i / \partial i$, is the difference of the electrical resistances of the two electrodes, and the activity of the two anodes can be compared from the current, i , at $\Delta E_i = 0$ volt. The tungsten addition enhanced the activity for oxygen evolution.

Keywords: Anode, oxygen evolution efficiency, durability, polarization, SEM

1. Introduction

For production of enormous amount of green hydrogen fuel based on seawater electrolysis, enormous amount of chlorine evolution, which generally occurs on the anode in seawater electrolysis, is not allowed [1-3]. Electrodeposited manganese oxide is known as the electrocatalyst for oxygen evolution without formation of chlorine in seawater electrolysis. Titanium metal has been used as the substrate for manganese oxide deposit. The present author prepared the electrocatalyst manganese dioxide by anodic deposition from Mn^{2+} aqueous solution. For prevention of insulating TiO_2 formation on the titanium substrate during anodic polarization we used the intermediate layer, which was generally IrO_2 , between the electrocatalyst and the substrate. Thus, the anode consisted of three layers of the top-most layer of the electrocatalyst, the intermediate IrO_2 layer and the titanium substrate. When the performance of the MnO_2 electrocatalyst without addition of other cations in 0.5 M NaCl at 1000 Am^{-2} that is the current density of industrial electrolysis, was examined more than 8% of electricity passed was consumed for chlorine formation and manganese dioxide itself suffered oxidative dissolution in the form of MnO_4^- [4]. This was in contrast to the report that the oxygen evolution efficiency was 99+% on a dimensionally stable anode covered with manganese deposited in seawater with 150 mg/l Mn^{2+} [5]. Hashimoto and his co workers add various cations to Mn^{2+} electrolytes during anodic deposition to prevent chlorine evolution and oxidative dissolution of the

electrocatalysts. The addition of Mo^{6+} [4, 6] and/or W^{6+} [7] was effective, showing the 100 % oxygen evolution efficiency. Formation of triple oxides, such as Mn-Mo-W oxides [8-10], Mn-Mo-Fe oxides [11, 12] and Mn-Mo-Sn oxides [13, 14] were particularly effective for extension of the lifetime of the anode. The electrocatalysts with Mo, W, Fe and/or Sn were all identified as a single phase multiple oxides of $\gamma\text{-MnO}_2$ structure, without forming any second oxide phase, and were stable without suffering from oxidative dissolution in the form of MnO_4^- in spite of the polarization potential far higher than the oxidation potential of MnO_2 to MnO_4^- [3]. The degradation of the anode is caused by partial detachment of electrocatalyst and oxidation of the titanium substrate during seawater electrolysis. The electrocatalysts for oxygen evolution are prepared by anodic deposition. The main reaction during anodic deposition is oxygen evolution because of preparation of the electrocatalyst for oxygen evolution. The deposition cannot occur on the portions of the surface covered with oxygen bubbles, and hence pores exist in the deposit. Oxygen evolution in electrolysis preferentially occurs at the bottoms of pores where the electrical resistance of deposit oxide is lower than the top surface of deposits. Thus destruction of deposit leading to partial detachment takes place from the bottoms of pores. The present author experienced that repeated deposition of Mn-Mo-Sn triple oxide electrocatalysts elongated the life of anode [13]. Detailed study of the performance of the anodes with Mn-Mo-Sn triple oxide electrocatalysts suggested that the repeated anodic deposition of electrocatalysts was effective to cover the pores [14]. In the present work repeated anodic

* Corresponding author. Tel.: +020181229082

Fax: 02034599520; E-mail: ahmed.abdelmoneim@ejust.edu.eg

© 2011 International Association for Sharing Knowledge and Sustainability

DOI: 10.5383/ijtee.04.01.005

deposition of Mn-Mo-W triple oxide electrocatalysts was attempted and the beneficial effects of tungsten on the performance of the anode were examined.

2. Experimental

2.1. Electrode preparation

The surface of titanium substrate net was roughened for an increase in the anchor effect of the intermediate layer and electrocatalysts by immersion in 11.5 M H_2SO_4 at $80^\circ C$ until hydrogen evolution was ceased. The surface-roughened titanium substrate was coated with the IrO_2 intermediate layer. For the formation of the IrO_2 layer, bluish coating of 0.52 M H_2IrCl_6 butanol solution on the titanium substrate, subsequent drying at $80^\circ C$ for 10 min and calcination at $450^\circ C$ for 10 min were repeated three times and the final calcination was continued for 60 min.

Analytically pure $MnSO_4 \cdot 5H_2O$, $Na_2MoO_4 \cdot 2H_2O$ and $Na_2WO_4 \cdot 2H_2O$ were used for preparation of electrocatalysts. A 0.2 M $MnSO_4$ -0.003 M Na_2MoO_4 -0.006 M Na_2WO_4 solution of pH 0.0 was used in continuous and repeated anodic deposition on the IrO_2 -coated titanium net at $600 Am^{-2}$ and $90^\circ C$. The electrocatalyst without tungsten was also prepared by anodic deposition in a 0.2 M $MnSO_4$ -0.003 M Na_2MoO_4 solution of pH 0.0 at $600 Am^{-2}$ and $90^\circ C$. The pH of the solution was adjusted by adding 18 M H_2SO_4 .

For repeated deposition, after deposition for every 30 min, the electrolyte was renewed and the surface of deposit was washed and dried.

2.2. Electrode characterization

The deposits were characterized by EPMA and X-ray diffraction of $CuK\alpha$ mode at a glancing angle, θ , of 5° .

2.3. Electrode performance

The performance of the electrode was examined by electrolysis of 0.5 M NaCl solutions of pH 8.7 at $1000 Am^{-2}$. The oxygen evolution efficiency was estimated by the difference between the total charge passed during electrolysis and the charge consumed for formation of chlorine analyzed by iodometric titration. The detailed method and accuracy of iodometric titration have been written elsewhere [12].

Polarization curves were measured in the galvanostatic mode, from low to high current densities, with about ten measurements within each decade. Each measurement lasted for 1 min. Correction for iR drop was made with a current-interruption technique. All electrochemical measurements were performed using an electrochemical cell of two compartment and three electrodes with platinum foil as an auxiliary electrode and $Ag/AgCl/KCl$ (sat.) as a reference electrode.

3. Results

In X-ray diffraction of all anodes deposited in 0.2 M $MnSO_4$ -0.003 M Na_2MoO_4 solutions with and without Na_2WO_4 only γ - MnO_2 type oxide was identified and no other diffraction lines of separate oxides of molybdenum and tungsten were observed. Consequently, the deposits were composed of a single phase of $Mn_{1-x-y}Mo_xW_yO_{2+x+y}$ triple oxide or the $Mn_{1-x}Mo_xO_{2+x}$ double oxide of the γ - MnO_2 type structure.

Figure 1 shows the oxygen evolution efficiency of anodes with $Mn_{1-x-y}Mo_xW_yO_{2+x+y}$ triple oxide electrocatalysts deposited

continuously and repeatedly at $600 Am^{-2}$ in 0.2 M Mn^{2+} -0.003 M Mo^{6+} -0.006 M W^{6+} solution of pH 0.0 and $90^\circ C$. The oxygen evolution efficiency of the $Mn_{1-x}Mo_xO_{2+x}$ double oxide electrocatalyst deposited continuously for 60 min at $600 Am^{-2}$ in 0.2 M Mn^{2+} -0.003 M Mo^{6+} solution without tungsten of pH 0.0 and $90^\circ C$ is also shown for comparison. The oxygen evolution efficiency of the $Mn_{1-x}Mo_xO_{2+x}$ double oxide anode becomes lower than 99% after electrolysis for about 150 h.

The oxygen evolution efficiency of the $Mn_{1-x-y}Mo_xW_yO_{2+x+y}$ triple oxide anode deposited for 30 min is higher than 99% for 320 h in spite of the fact that the thickness of the $Mn_{1-x-y}Mo_xW_yO_{2+x+y}$ triple oxide anode formed by deposition for 30 min was $8.0 \mu m$, whereas the thickness of the $Mn_{1-x-y}Mo_xO_{2+x}$ double oxide anode formed by deposition for 60 min was $15.7 \mu m$.

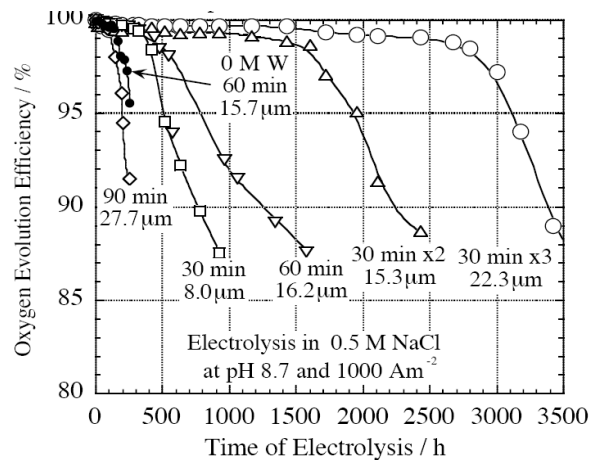
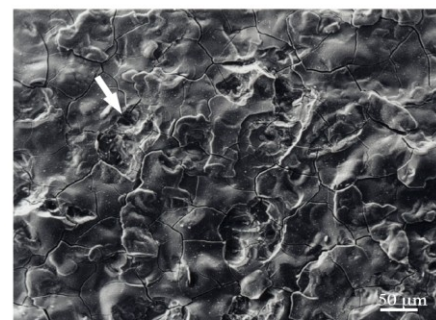


Fig.1. Change in oxygen evolution efficiency of the anodes with $Mn_{1-x-y}Mo_xO_{2+x}$ double oxide and $Mn_{1-x-y}Mo_xW_yO_{2+x+y}$ triple oxide electrocatalysts in electrolysis of 0.5 M NaCl solution of pH 8.7 at $1000 Am^{-2}$.



(a)



(b)

Fig.2. SEM images of $Mn_{1-x-y}Mo_xO_{2+x}$ double oxide anode (a) and $Mn_{1-x-y}Mo_xW_yO_{2+x+y}$ triple oxide anode (b) deposited for both 60 min.

Figure 2 shows SEM images of $Mn_{1-x}Mo_xO_{2+x}$ double oxide anode (a) and $Mn_{1-x-y}Mo_xW_yO_{2+x+y}$ triple oxide anode (b). A high density of cracks is observed. However, as can be seen from the fact that there is no relationship between cracks and deposit structure, that is, mostly unevenness, cracks did not exist during electrolysis but were formed as a result of rapid evacuation and drying of the wet anode in the scanning electron microscope.

As an arrow indicates a pore, there are high density of pores in the $Mn_{1-x}Mo_xO_{2+x}$ double oxide, which are responsible for destruction and partial detachment of the electrocatalyst. For the formation of the electrocatalysts the oxygen evolution is the competitive reaction with the anodic deposition, and no deposit growth occurs on the oxygen bubbles adsorbing on the deposit surface during deposition. Thus, anodic deposition leaves pores in the deposit. As can be seen in Fig.2 (b) the tungsten addition significantly decreased the density of pores. The lower density of pores prevents easy partial detachment of the deposit by high pressure of hydrogen at the bottoms of pores and provides the longer life of the $Mn_{1-x-y}Mo_xW_yO_{2+x+y}$ triple oxide anode in comparison with that of the $Mn_{1-x}Mo_xO_{2+x}$ double oxide anode.

As shown in Fig. 1, elongation of deposition time to 60 min was not sufficient, the oxygen evolution efficiency higher than 99 % being kept only 480 h. However, further extension of the deposition time to 90 min does not extend but decreases the life. Prolonged continuous deposition forms unnecessarily thick deposit with deep pores responsible for shorter life [12]. In contrast, when deposition was repeated every 30 min using the washed and dried specimen and the fresh electrolyte, the $Mn_{1-x-y}Mo_xW_yO_{2+x+y}$ triple oxide anode deposited for 30 min two times shows the oxygen evolution efficiency higher than 99% for more than 1500 h. Furthermore, the $Mn_{1-x-y}Mo_xW_yO_{2+x+y}$ triple oxide anode deposited for 30 min three times reveals the oxygen evolution efficiency higher than 99 % exceeding 2600 h.

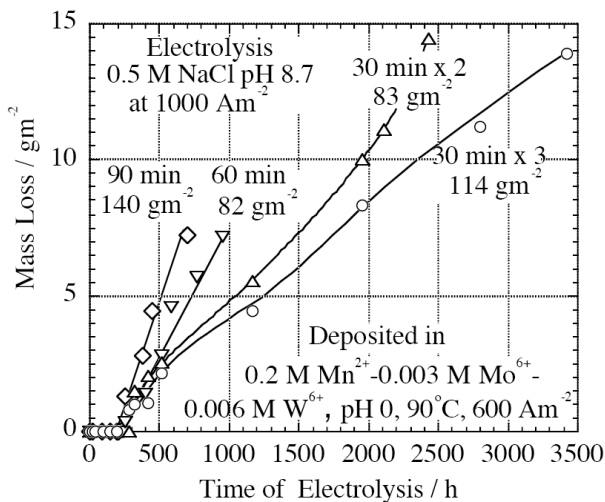


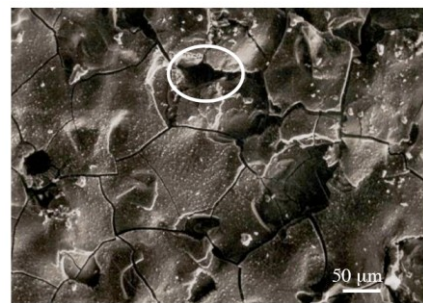
Fig.3. Mass loss of continuously and repeatedly deposited $Mn_{1-x-y}Mo_xW_yO_{2+x+y}$ triple oxide electrocatalyst anodes during electrolysis at 1000 Am^{-2} in 0.5 M NaCl at pH 8.7.

Figure 3 shows the mass loss of the anodes during electrolysis of 0.5 M NaCl solution at pH 8.7. After electrolysis for 250 h the mass loss begins to appear for the anodes deposited for 90 and 60 min. Although the appearance of the mass loss for the anodes deposited 30 min two and three times was delayed, their mass losses were detected after electrolysis for about 300 h. In

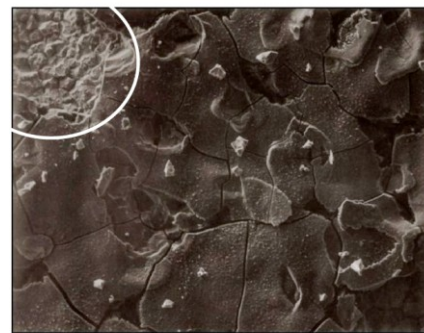
this manner, the mass loss was detected for all anodes within about 300 h. However, repeated deposition suppresses the mass loss and the slower the increasing rate of mass loss, the longer the life of the anode.

Figures 4 (a) and (b) show scanning electron micrographs of the anode deposited for 30 min three times after electrolysis for 1000 and 3450 h, respectively. After electrolysis for 1000 h, a partial detachment of the top-most layer took place as surrounded by a white circle. After electrolysis for 3450 h, complete detachment of three layers of deposits can be seen in the upper-left surrounded by a white circle in addition to portions where a top-most layer or a top-most layer and the second layer were detached. As well as cracking, scattering of fragments of the electrocatalyst occurred as a result of evacuation and drying of the wet anode in the scanning electron microscope.

Figures 3 and 4 illustrate that partial detachment from bottoms of pores of the top-most layer begins to occur after electrolysis for several hundred hours. However, repeated deposition was able to cover the pores of the underlying deposits. Thus, if repeated deposition was performed, the oxygen evolution efficiency was maintained until all deposit layers were partially detached.



(a)



(b)

Fig.4. SEM images of the $Mn_{1-x-y}Mo_xW_yO_{2+x+y}$ triple oxide anode deposited for 30 min three times after electrolysis of 0.5 M NaCl at pH 8.7 and 1000 Am^{-2} for 1000 h (a) and 3450 h (b).

The effects of tungsten addition and repeated deposition on the oxygen evolution behavior were examined electrochemically. Figure 5 shows galvanostatic polarization curves of the $Mn_{1-x-y}Mo_xW_yO_{2+x+y}$ triple oxide anode deposited for 30 min and the $Mn_{1-x}Mo_xO_{2+x}$ double oxide anode deposited for 60 min measured in 0.5 M NaCl solution at pH 8.7. These two anodes show different polarization curves.

Regardless of the anode material whether it is oxide or metal, the relation of current density, i , with the overpotential for

oxygen evolution, E_{reaction} , is expressed as

$$E_{\text{reaction}} = b (\log i - \log i_0) \quad (1)$$

Where i_0 is the current density at $E_{\text{reaction}} = 0$ volt and b is the Tafel slope. The Tafel slopes change with the reaction mechanism and i_0 changes with the activity of anode and the reaction mechanism. When the electrical resistance of the oxide anode is not negligible, before the current for splitting oxygen from water reaches the anode surface through the electrocatalyst, the potential drop, $E(r)_i$, occurs by passage of current, i , through the body of oxide anode, whose electrical resistance is r . $E(r)_i$ is written as:

$$E(r)_i = ri \quad (2)$$

Thus, the overpotential for oxygen evolution, E_{reaction} , is lower by $E(r)_i$ than the observed potential, E_{observed} .

$$E_{\text{observed}} = E_{\text{reaction}} + E(r)_i \quad (3)$$

The observed potential can be written as

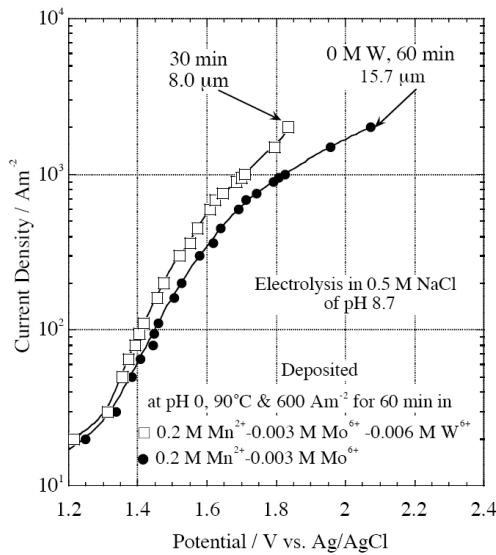


Fig.5. Galvanostatic polarization curves of anodes with $Mn_{1-x-y}Mo_xW_yO_{2+x+y}$ triple oxide deposited for 30 min and $Mn_{1-x-y}Mo_xO_{2+x}$ double oxide deposited for 60 min measured in 0.5 M NaCl at pH 8.7.

$$E_{\text{observed}} = E_{\text{reaction}} + E(r)_i = b (\log i - \log i_0) + ri \quad (4)$$

In other words, the electrode potential observed is the sum of the overpotential for oxygen evolution and the potential drop based on the electrical resistance of the anode. If the oxygen evolution reaction on two different anodes, A and B, occurs by the same mechanism, that is, the same Tafel slope, b , the difference in potentials, ΔE_i , observed between two anodes at individual current density, i , will be

$$\Delta E_i = E_{\text{observed}}(A)_i - E_{\text{observed}}(B)_i = b (\log i_{0B} - \log i_{0A}) + (r_A - r_B) i \quad (5)$$

Where r_A and r_B are electrical resistances of anodes A and B.

$$\text{Then } i = \Delta E_i / (r_A - r_B) + b (\log i_{0A} - \log i_{0B}) / (r_A - r_B)$$

If the $\Delta E_i - i$ plot shows a straight line, the mechanism of the electrochemical reaction on the two anodes is the same as each other, and the gradient, $\partial(\Delta E_i) / \partial i$, corresponds to the resistance difference between two anodes

$$\partial(\Delta E_i) / \partial i = r_A - r_B \quad (6)$$

From Equation (5) at $\Delta E_i = 0$ volt

$$i(\Delta E_i=0) = b (\log i_{0A} - \log i_{0B}) / (r_A - r_B) \quad (7)$$

Thus the activities of two electrodes, i_{0A} and i_{0B} can be compared from the current density, i , at $\Delta E_i = 0$ volt.

In Fig. 5, the $Mn_{1-x-y}Mo_xW_yO_{2+x+y}$ triple oxide anode shows lower potentials than the $Mn_{1-x-y}Mo_xO_{2+x}$ double oxide anode at individual current density.

The potentials of the $Mn_{1-x-y}Mo_xW_yO_{2+x+y}$ triple oxide anode were subtracted from those of the $Mn_{1-x-y}Mo_xO_{2+x}$ double oxide anode at individual current density. Figure 6 shows the $\Delta E_i - i$ relation. The $\Delta E_i - i$ plot shows a straight line. Thus, the mechanism of oxygen evolution, that is, Tafel slope, b , for the $Mn_{1-x-y}Mo_xW_yO_{2+x+y}$ triple oxide anode and the $Mn_{1-x-y}Mo_xO_{2+x}$ double oxide anode is the same as each other, and we can estimate the resistance difference of two oxide anodes from

$$\partial(\Delta E_i) / \partial i = r^{0.006 MW}_{60 \text{ min}} - r^{0.006 MW}_{30 \text{ min}} > 0 \quad (8)$$

The resistance difference, $\partial(\Delta E_i) / \partial i$, is mostly based on the difference in the thicknesses of deposits, because the deposition time of the $Mn_{1-x-y}Mo_xO_{2+x}$ double oxide was 60 min but that of the $Mn_{1-x-y}Mo_xW_yO_{2+x+y}$ triple oxide was 30 min.

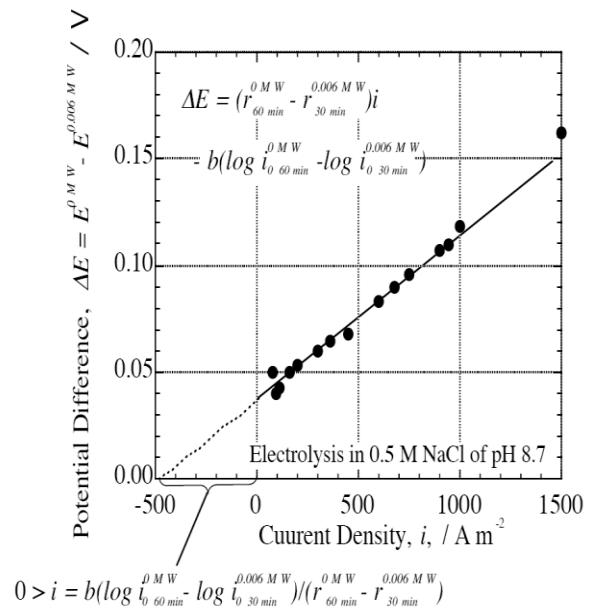


Fig.6. Potential difference between two polarization curves shown in Fig. 5 as a function of current density.

On the other hand, the current density, i , at $\Delta E_i = 0$ volt is negative. From equation (7)

$$0 > i(\Delta E_i=0) = b (\log i^{0.006 MW}_{60 \text{ min}} - \log i^{0.006 MW}_{30 \text{ min}}) / (r^{0.006 MW}_{60 \text{ min}} - r^{0.006 MW}_{30 \text{ min}}) \quad (9)$$

Thus, $\log i^{0.006 MW}_{30 \text{ min}} > \log i^{0.006 MW}_{60 \text{ min}}$ (10) Consequently, the activity of the $Mn_{1-x-y}Mo_xW_yO_{2+x+y}$ triple oxide anode for oxygen evolution is higher than that of the $Mn_{1-x-y}Mo_xO_{2+x}$ double oxide anode. Because the activity is dependent upon the composition of the top-most surface of the anode, it can be concluded that the tungsten addition enhances the activity for oxygen evolution.

Figure 7 shows galvanostatic polarization curves measured in 0.5 M NaCl at pH 8.7 for various $Mn_{1-x}W_xMo_yO_{2+x+y}$ triple oxide anodes deposited continuously and repeatedly. The anode deposited for 30 min shows the lowest potential at individual current density. The potentials of the anode deposited for 30 min were subtracted from those of all other anodes shown in Fig. 8 at individual current density. Figure 8 shows the ΔE_i - i relations. All ΔE_i - i plots show straight lines. Thus, we can estimate the resistance difference of two oxide anodes from

$$\partial(\Delta E_i)/\partial i = r - r_{30 \text{ min}} \quad (11)$$

All potential differences, $\partial(\Delta E_i)/\partial i$, are positive. The positive potential differences between the $Mn_{1-x}W_xMo_yO_{2+x+y}$ triple oxide anodes are mostly based on the difference in the thicknesses of deposits. For instance

$$r_{30 \text{ min} \times 3} - r_{30 \text{ min}} > r_{30 \text{ min} \times 2} - r_{30 \text{ min}} > 0 \quad (12)$$

Thus,

$$r_{30 \text{ min} \times 3} > r_{30 \text{ min} \times 2} > r_{30 \text{ min}} \quad (13)$$

Similarly,

$$r_{90 \text{ min}} - r_{30 \text{ min}} > r_{60 \text{ min}} - r_{30 \text{ min}} > 0 \quad (14)$$

Thus,

$$r_{90 \text{ min}} > r_{60 \text{ min}} > r_{30 \text{ min}} \quad (15)$$

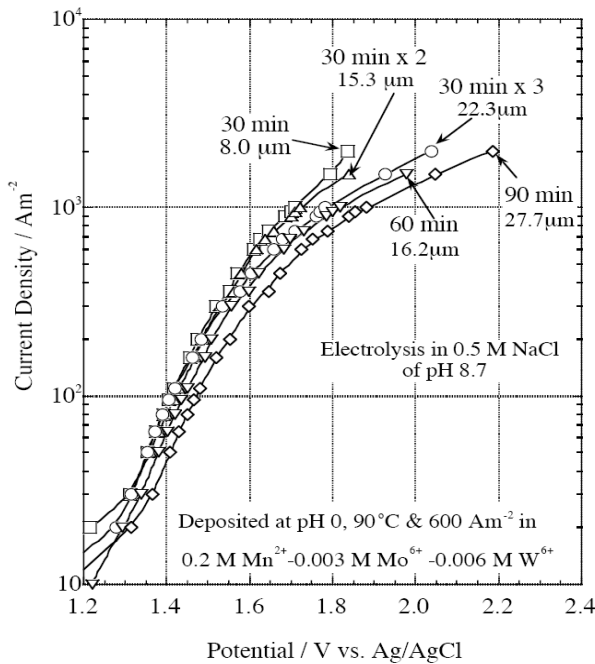


Fig.7. Galvanostatic polarization curves of continuously and repeatedly deposited $Mn_{1-x}W_xMo_yO_{2+x+y}$ triple oxide anodes measured in 0.5 M NaCl at pH 8.7.

The current densities, i , at $\Delta E_i = 0$ volt for $E_{30 \text{ min} \times 2} - E_{30 \text{ min}}$ and $E_{30 \text{ min} \times 3} - E_{30 \text{ min}}$

$$i(\Delta E_i=0) = \frac{b(\log i_{0 \text{ 30 min} \times 2} - \log i_{0 \text{ 30 min}})}{r_{30 \text{ min} \times 2} - r_{30 \text{ min}}} = \frac{b(\log i_{0 \text{ 30 min} \times 3} - \log i_{0 \text{ 30 min}})}{r_{30 \text{ min} \times 3} - r_{30 \text{ min}}} = 0 \quad (16)$$

Thus, the activities of three anodes for oxygen evolution, $i_{0 \text{ 30 min} \times 3}$, $i_{0 \text{ 30 min} \times 2}$ and $i_{0 \text{ 30 min}}$ are the same as each other.

$$i_{0 \text{ 30 min}} = i_{0 \text{ 30 min} \times 2} = i_{0 \text{ 30 min} \times 3} \quad (17)$$

The activity is determined by the composition of the top-most surface, and the compositions of the top-most surfaces of the three deposits formed by deposition for final 30 min from the fresh solution are not different.

Although the electrical resistances of these three anodes are different, $r_{30 \text{ min} \times 3} > r_{30 \text{ min} \times 2} > r_{30 \text{ min}}$, because of different thicknesses, the composition of the top-most surface was not affected by a decrease in the overpotential for anodic deposition, E_{reaction} , as a result of increasing the potential drop, $E(r)_i$.

On the other hand, the activity decreased by continuous deposition for longer time.

$$i_{0 \text{ 30 min}} = i_{0 \text{ 30 min} \times 2} = i_{0 \text{ 30 min} \times 3} > i_{0 \text{ 60 min}} > i_{0 \text{ 90 min}} \quad (18)$$

The activity of anode for oxygen evolution is determined by the composition of the top-most surface of the anode. Figure 9 shows the EPMA results of molybdenum and tungsten in the anode surface as a function of time of deposition. The EPMA results show the decrease in both tungsten and molybdenum in the deposit with time of anodic deposition. Consequently, the prolonged continuous deposition leads to the decrease in tungsten and molybdenum contents in the deposits and to the decrease in the activity of the anode for oxygen evolution.

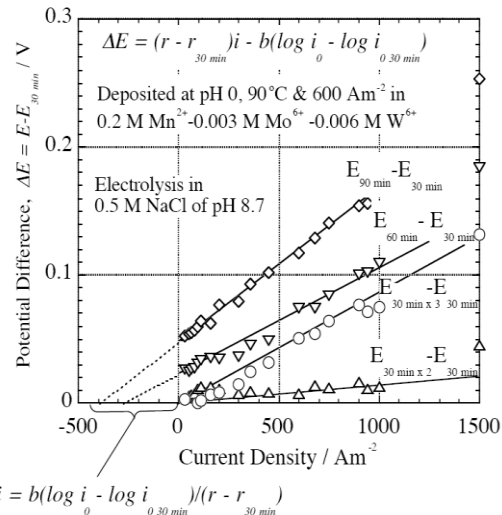


Fig.8. Potential differences obtained by subtraction of the polarization curve of the $Mn_{1-x}W_xMo_yO_{2+x+y}$ triple oxide deposited for 30 min from those of other $Mn_{1-x}W_xMo_yO_{2+x+y}$ triple oxide anodes shown in Fig. 7 as a function of current density.

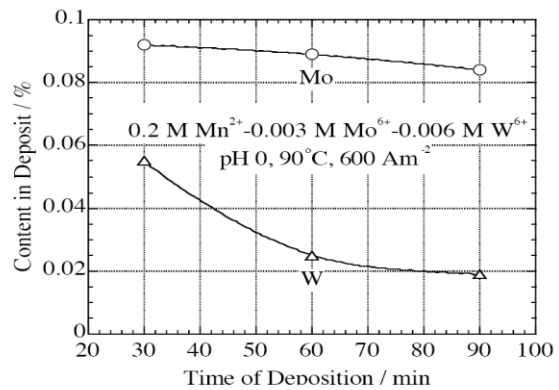


Fig. 9. EPMA results of molybdenum and tungsten contents in electrocatalysts deposited in 0.2 M Mn^{2+} -0.003 M Mo^{6+} -0.006 M W^{6+} solution of pH 0.0 as a function of time of anodic deposition.

Conclusions

$Mn_{1-x-y}Mo_xW_yO_{2+x+y}$ triple oxide electrocatalysts for the anode producing oxygen without forming chlorine in seawater electrolysis were prepared by anodic deposition from $MnSO_4-Na_2MoO_4-Na_2WO_4$ solutions. The performance of the anode for oxygen evolution in 0.5 M NaCl solutions was examined at 1000 Am^{-2} . The following conclusions were drawn:

- The tungsten addition decreased the density of pores responsible for partial detachment of electrocatalysts, which occurs by high pressure of oxygen formed preferentially at the bottom of pores during electrolysis, and the tungsten addition extended the life of the anode.
- Repeated anodic deposition of the electrocatalyst using the fresh solution and the specimen washed and dried was able to cover the pores in the underlying electrocatalysts.
- Destruction of the repeatedly deposited anodes occurred by partial detachment of the top-most layer of the electrocatalyst by high pressure of oxygen at the pore bottom of the top-most layer, and a high oxygen evolution efficiency was kept until all deposited layers were partially detached. Thus, the repeated deposition significantly extended the life of the anode.
- The potential observed in anodic polarization of an oxide electrode was the sum of the overpotential of the electrochemical reaction and the potential drop as a result of passage of current through the oxide whose electrical resistance was not negligibly small.
- If the mechanism of the electrochemical reaction on two oxide anodes is the same as each other, the relation of the potential difference of two anode at individual current, ΔE_i , with the current, i , should show the straight line: The gradient, $\partial \Delta E_i / \partial i$, is the difference of the electrical resistances of the two electrodes, and the activity of the two anodes can be compared from the current, i , at $\Delta E_i = 0$ volt.

Acknowledgments

The author would like to express his sincere gratitude to Emeritus Professor Dr. Koji Hashimoto of Tohoku Institute of Technology, Sendai, Japan for providing the research facilities of coating, XRD measurements and an opportunity to visit Tohoku Institute of Technology, Japan as a Visiting Research Fellow supported by Daiki Atika Engineering Co. Ltd., Japan.

References

- [1]. <http://www.eia.doe.gov/fueloverview.html>
- [2]. K. Hashimoto, *Met. Technol.*, **63**(7), 5 (1993).
- [3]. [3] K. Hashimoto, M. Yamasaki, K. Fujimura, T. Matsui, K. Izumiya, M. Komori, A. A. El-Moneim, E. Akiyama, H. Habazaki, N. Kumagai, A. Kawashima and K. Asami, *Mater. Sci. Eng.* **A267**, 200 (1999).
- [4]. J. E. Bennett, *Int. J. Hydrogen Energy*, **5**, 401 (1980). [doi:10.1016/0360-3199\(80\)90021-X](https://doi.org/10.1016/0360-3199(80)90021-X)
- [5]. K. Fujimura, K. Izumiya, A. Kawashima, H. Habazaki, E. Akiyama, N. Kumagai and K. Hashimoto, *J. Appl. Electrochem.*, **29**, 765 (1999). [doi:10.1023/A:1003492009263](https://doi.org/10.1023/A:1003492009263)
- [6]. K. Fujimura, T. Matsui, K. Izumiya, N. Kumagai, E. Akiyama, H. Habazaki, A. Kawashima, K. Asami and K. Hashimoto, *Mater. Sci. Eng.*, **A267**, 254 (1999). [doi:10.1016/S0921-5093\(99\)00100-8](https://doi.org/10.1016/S0921-5093(99)00100-8)
- [7]. K. Izumiya, E. Akiyama, H. Habazaki, N. Kumagai, A. Kawashima and K. Hashimoto, *Electrochimica Acta.*, **43**, 3303 (1998). [doi:10.1016/S0013-4686\(98\)00075-9](https://doi.org/10.1016/S0013-4686(98)00075-9)
- [8]. H. Habazaki, T. Matsui, A. Kawashima, K. Asami, N. Kumagai and K. Hashimoto, *Scripta Mater.*, **44**, 1659 (2001). [doi:10.1016/S1359-6462\(01\)00876-4](https://doi.org/10.1016/S1359-6462(01)00876-4)
- [9]. H. Habazaki, T. Matsui, A. Kawashima, K. Asami, N. Kumagai and K. Hashimoto, *J. Appl. Electrochem.*, **32**, 993 (2002). [doi:10.1023/A:1020912611494](https://doi.org/10.1023/A:1020912611494)
- [10]. A. A. El-Moneim, N. Kumagai, K. Asami and K. Hashimoto, *Materials Trans.*, **46**, 309 (2005). [doi:10.2320/matertrans.46.309](https://doi.org/10.2320/matertrans.46.309)
- [11]. N. A. Abdel Ghany, N. Kumagai, S. Meguro, K. Asami and K. Hashimoto, *Electrochimica Acta.*, **48**, 21 (2002). [doi:10.1016/S0013-4686\(02\)00539-X](https://doi.org/10.1016/S0013-4686(02)00539-X)
- [12]. N. A. Abdel Ghany, S. Meguro, N. Kumagai, K. Asami and K. Hashimoto, *Materials Trans*, **44**, 2114 (2003). [doi:10.2320/matertrans.44.2114](https://doi.org/10.2320/matertrans.44.2114)
- [13]. A. A. El-Moneim, N. Kumagai, K. Asami, and K. Hashimoto, *ECS Trans.*, **1**(4), 491 (2006).
- [14]. A. A. El-Moneim, J. Bhattarai, Z. Kato, K. Izumiya, N. Kumagai, K. Hashimoto *ECS Trans.*, **25**(40), 127 (2010). [doi:10.1149/1.3422589](https://doi.org/10.1149/1.3422589)